Transradial Amputee Reaching: Compensatory Motion Quantification Versus Unaffected Individuals Including Bracing

Adam J. Spiers, *Member*, *IEEE*, Yuri Gloumakov, *Member*, *IEEE*, and Aaron M. Dollar, *Senior Member*, IEEE

***Abstract*—Joint absence in people with upper-limb-difference leads to compensatory motions. Such compensation has long been a topic of study, but typically only for a single object/user layout, which is unlikely to spatially generalize. We seek to understand how motion varies over a planar workspace for different target orientations and wrist mobility conditions. We therefore present a study that records arm and torso pose during grasping of 49 equally spaced cylindrical targets. Furthermore, we seek to validate the research practice of using wrist-immobilizing bypass sockets on able-bodied participants to simulate prostheses without wrists. Participants were 2 transradial amputees and 7 able-bodied individuals who conducted the study with and without wrist braces, generating 2450 trajectories. Heat-maps illustrate variation over the workspace in Mean Joint Angle, Range of Joint Motion and Distance Travelled by Body Segment. Results indicate that greater wrist restriction primarily exacerbated shoulder internal rotation and elbow flexion, not the trunk. We observed that bypass sockets do not fully simulate amputee behavior. Furthermore, amputee reaching with their intact limb is different to the reaching motion of normative participants, implying that transradial limb-difference affects both sides of the body. Differences in participant behavior were also observed between horizontal and vertical target orientations.**

***Index Terms*— manipulation, human motion analysis, upper-limb, prosthetics.**

I. Introduction

The field of upper-limb prosthetics is often focused on the development of more dexterous artificial hands, with enhanced grasping capabilities. Another key aspect of manipulation is the ability to adequately locate one's hand or gripper within the workspace, to execute the desired grasp or action on an object.

Although the wrist is absent in many amputees, fairly little attention has been given to its prosthetic development [1]. Instead, above-wrist amputees are often fitted with a prosthetic device that either does not include a wrist or includes only a passive pronation/supination mechanism that must be rotated using the intact limb or an environmental feature. When attempting to use the prosthesis during reaching and grasping tasks, the forearm is essentially locked into a single orientation.

For transradial (or more proximal) upper-limb amputees, the absence of wrist joints means that setting the final orientation of the hand must be achieved by other degrees of freedom (DOF), such as those of the shoulder and trunk. This method is known as compensatory motion, given that unconventional body joints are employed to compensate for the lack of others. Compensatory movements can place additional stresses on the remaining joints and lead to overuse complications [2], [3].

Novel prosthetics systems are frequently evaluated by able-bodied persons using bypass sockets [4]–[6]. Bypass sockets are a mechanical interface that enables a terminal device to be mounted to the forearm of an able-bodied person (bypassing the 2 distal wrist joints). The use of bypass sockets assumes that both able-bodied persons with sockets and TR amputees will move in a similar fashion. To our knowledge, a formal comparison has not been previously made, though one study did compare two end-effector configurations of prosthesis simulators to able-bodied participants [7].

Reaching movement evaluation and comparison is typically performed with only a single configuration of user and target, often within the framework of activities of daily living (ADLs) [2], [3], [8], [9]. ~~One example study involved participants is turning over a piece of paper [10], in the constraints of the SHAP test [11].~~ Clearly, daily life is not so structured, with reaching targets scattered around the workspace in locations that may lead to increased or decreased compensation requirements. One common ADL example is when grocery shopping, where items are spread horizontally and vertically across store shelving (Fig. 1).

In this work we attempt to achieve a more holistic understanding of human compensatory motions by recording reaching motion across multiple points of a workspace that is consistent with taking items from a shelf. We then vary the wrist mobility conditions of the user to study the effect of each condition on compensatory behaviors, via joint and body segment analysis. Our goal is to discover and quantify how reaching movement is impacted by wrist conditions across regions of a user's workspace. Parameters have been similarly modelled across discretely sampled robot manipulators to better understand spatial-aspects of performance [10]. We hope that the information we have determined may be used to improve

A. J. Spiers is with The Department of Electrical and Electronic Engineering, Imperial College London, London, UK (email: a.spiers@imperial.ac.uk). Y. Gloumakov is with the Mechanical Engineering Department, University of California, Berkeley, CA 94720 USA (email: yurigloum@berkeley.edu). A.M. Dollar is with the Mechanical Engineering and Materials Science Department, Yale University, New Haven, CT 06511 USA (email: aaron.dollar@yale.edu).

Figure 1. Supermarket shelving is a common environment that requires reaching to multiple target locations in an individual's workspace (image from Alamy.com)

prosthetic devices and training, while also potentially aiding the design of spaces to reduce complications related from compensatory motions.

We simulated grasping of common objects (e.g. cup, cans, etc.) at various heights and lateral displacements from a participant's body by using a 7x7 equally (0.3m) spaced grid of vertically and horizontally oriented cylindrical targets (plastic poles) that were placed in front of the participants (Fig. 2). It may be noted that rather than studying single grasps of a wide variety of objects in an attempt to represent daily life (as in a SHAP test) we instead focused on grasping a single generic object many times at various locations and orientations. Though it would be possible (and interesting) to repeat the study with different target objects (e.g. of different size or shape) this would greatly extend the length of the study for participants and so was not implemented at this time.

Able-bodied participants reached to all points on the grid both unimpaired and whilst wearing two types of wrist brace that limits wrist motion by 2DOF and 3-DOF. Transradial Amputee participants reached to targets using their dominant hand and their prosthetic hand. Actions were recorded using a Vicon motion capture system.

Due to the large number of recorded reaching trajectories, over several conditions, we opt to present our results using a 'heat-map' based representation of scalar metrics extracted from each trajectory (Fig. 3). Such heat-maps offer spatial comparison of variable output across the workspace and across conditions. Further statistical analysis gives these results a numerical output. We explore variabilities between subjects and reaching conditions, highlighting joint compensation similarities across able-bodied and amputee participants.

This paper builds upon the authors' previous work in which a preliminary investigation compared reaching motions of able-bodied participants to vertical cylindrical targets while their wrist was either constrained or unconstrained with a single 2DOF brace [11]. We expand on that work by:

- Increasing the number of able-bodied subjects from 4 to 7.
- Including 2 transradial amputees.
- Including both 2DOF and 3DOF braces (this was previously just 2DOF).
- Studying both vertical and horizontal targets, which require different grasp orientations.

Figure 2. Experimental setup with a transradial limb-different participant. Participants were requested to sequentially power-grasp 7 x 7 equally spaced targets on the beams of the grid. The image shows the target grid in horizontal configuration The experiment was repeated with the grid rotated 90 degrees into a vertical configuration. This rotation alters the target grasp orientation.

One transradial amputee uses a powered wrist mechanism and one has a passive wrist. The powered wrist was operated using electromyography (EMG) sensors embedded within the user's socket, while the passive wrist user would manually rotate the end effector using their other hand.

II. Related Work

Although upper-limb end effector and joint trajectories are under-constrained, able-bodied participants often move along consistent paths [12], [13] with predictable error bounds (e.g. [14]). When DOF of the upper limb are absent, compensation to these patterns emerge. Past works (e.g. [2], [3], [8], [9], [14]–[17]) have made efforts to numerically highlight compensatory motions in people with impaired wrist mobility. In these studies, participants' movements were often quantified using a motion capture system while they simulated various ADL. Metrics such as mean angle [8] and joint range of motion (ROM) [2], [3], [9], [14], [15] are used to assess differences.

Assessment of manipulation capabilities is typically performed using a standardized simulated ADL protocol, such as the Southampton Hand Assessment Protocol (SHAP) [18] that has been featured in a variety of motion studies. For example, comparison of joint motions and compensatory motions between unimpaired participants and those with a previous wrist injury was made using the page-turning task in the SHAP [14]. Researchers used joint ROM to quantitatively illustrate how impaired participant joint motion was typically outside the range of unimpaired participants.

In one study, trunk and head ROM were used to assess movement differences between able-bodied and amputee prosthesis-users [3]. Trunk, shoulder, and elbow ROM were tracked during selected SHAP tasks in a similar study [15].

Wrist splints have been previously used to constrain or partially limit participant wrist mobility along a combination of pronation/supination, flexion/extension, and radial/ulnar

deviation axes [2], [8], [17]. In one study, participant wrist and finger motions were restricted while they completed the SHAP

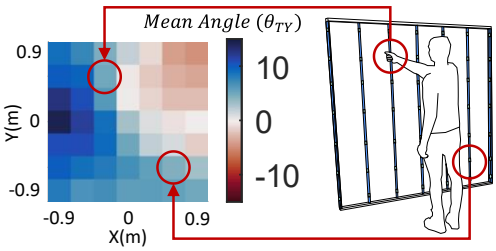

Figure 3. Metrics are represented as 'heat maps', with each square corresponding to joint/body segment behavior while reaching to a spatially equivilant target location on the grid (as viewed from the perspective of the participant).

test [3].

The Jebsen hand function test is another standardized test protocol that has been used to assess participant motion [17]. In that work, statistically significant differences between upper-limb and trunk motions were only present in certain tasks.

In another study on compensatory motion, mean joint angles were calculated while participants were tasked with removing an object from a box while donning a wrist splint [8].

Recently, increased interest has been shown with regard to multi-DOF actuated prosthetic wrists, as a means of improving reaching ability for upper-limb amputees [1], [6], [19], [20]. Indeed, compelling arguments have been made that the inclusion of articulated wrists may benefit upper limb prosthesis users more than multi-grasp prosthetic hands [2]. It is clear that intuitive user control of such wrists is a challenge that remains to be solved [1], [21]. leading to wrist omission in many prosthetic systems. The potential for variation in wrist DOF as a result of various prosthetic hardware influenced the decision to include 2DOF and 3-DOF wrist splints in this work.

The goal of our work is to better inform the design and choices of new prosthetic devices and interventions by studying the effects wrist impairments have on body compensation. A similar approach has been implemented in a study investigating different prosthetic wrist modules in amputees [9], where the shoulder joint was used to track compensatory motion. We additionally investigate the viability of using a wrist brace as an accurate simulation of prosthesis use by comparing the motion characteristics of participants with intact limbs wearing a wrist brace to those with affected limbs and transradial prosthesis.

In many of the works we have cited we noted a shortcoming in that the motions under observation are very specific and only studied in one configuration of the user and object. For example, turning the page of a book or removing an object from a box. In our work we wished to study a more general reaching motion that will be used across various workspace targets as standard, which motivates our grid of reaching targets. This approach clearly brings with it the complication of dimensionality. While prior work deals with only a single object/user configuration, we have 49 (7x7) per study condition. We therefore developed the heat map representation of Fig. 3 as a way of displaying variation in motion across a discretely sampled cartesian space. Though our experiment could also have had a depth component, this 3rd dimensions would have led to 343 reaching targets per study condition (assuming that we maintain the pattern of 7 intervals), and a 3D visualization that would be challenging to visually interpret.

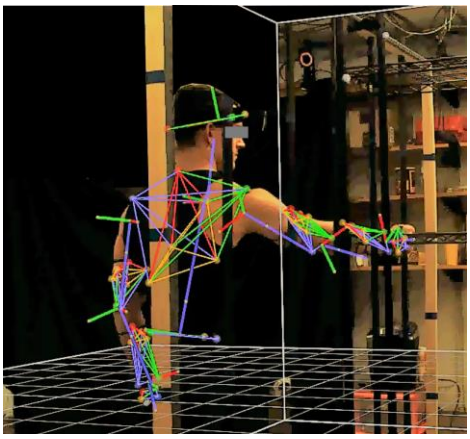

Figure 4: An able-bodied participants reaching to a target on the vertical grid setup with motion capture skeleton overlay. The image was created using a *VICON Bonita* reference camera with low color depth, which is why the black poles of the target grid (shown in Fig. 2) are not clearly visible.

III. Methods

This study protocol was approved by Yale University Institutional Review Board, HSC# 1610018511.

A. Study Apparatus

We placed 49 equally spaced targets in a 7x7 square grid at 0.3m intervals horizontally and vertically for participants to reach. The grid was constructed using a wooden frame (cross section of 20x30mm) rigged with five parallel plastic PVC pipes (25mm diameter) (Fig. 2). The grid is suspended 0.175m above the floor using a modular shelving unit and vice grips. The pipes were wrapped with black matte tape to minimize infrared reflections in the motion capture environment. Participants were tasked with reaching and grasping different target locations marked with blue *painter's tape* along the pipes and wooden structure.

The grid was used in both a vertical pipe orientation and a horizontal one by rotating the grid 90 degrees and resuspending it on the holding structure. Vertical pipe arrangement simulated grasping objects like cups, bottles, and tins from different shelf heights in a kitchen or supermarket, while a horizontal arrangement simulated grasping things like drawer handles. The dependance of wrist pronation/supination in switching between such grasps motivated our decision to include both grasp orientations in the study, as alternative compensatory motion approaches were likely to be required.

Participant motions were captured using 12 Vicon Bonita cameras (Vicon, Oxford, UK) arranged symmetrically and at different heights around the room, with the grid placed in the center. A reference video camera is integrated to the Vicon

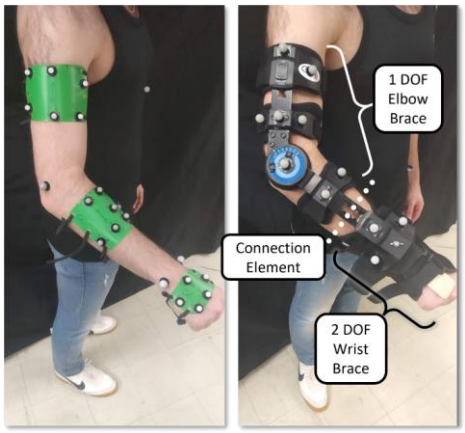

Figure 5: Left: the motion cluster markers used on the arms of *Intact* participants. Right: A custom bracing system was created by combining a commerical elbow brace with a commercial wrist orthosis, modificed with an additional wooden insert to limit wrist flexion/extension. This arrangment can optionally limit 2DOF or 3DOF of the wrist by detaching the connection element.

system and was used for inspecting the data during gap repair (Fig. 4 was produced with this camera).

Participants were suited with a sleeveless skin-tight (Nylon/Lycra blend) sports tank top in their size, adorned with retroreflective markers, placed around key locations on their pelvis, torso, and upper-limb according to [22]. Markers were affixed to the tank top or directly over the skin at select bony landmarks with double-sided adhesive tape. 'Clusters' of markers were additionally affixed to the humerus, forearm, and back of the hand (see Fig. 5) using thin flexible plastic and elastic straps. A piece of double-sided tape was placed underneath each marker cluster to prevent slipping against the skin. Head markers were affixed to an elastic sports headband. Marker 'clusters' were used for both joint angle calculation as well as in aiding reconstruction of obstructed markers lost by the Vicon system; obstruction was expected due to the large motion ranges and workspace of this study. Joint angles were calculated using the markers according to [22]. For participants that were using a prosthetic device, upper-limb markers were placed on analogous hand, wrist, forearm, and elbow landmarks (Fig. 6).

Two types of wrist braces were constructed for the able-bodied participants, one that restricted 2DOF (flexion/extension and ulnar/radial deviation) and one that restricted all 3DOF (including pronation/supination) of the wrist (Fig. 5). The brace features an aluminum internal structure (DonJoy ComfortFORM Wrist Support Brace – DJO Global, Vista CA, USA) that limits wrist flexion/extension and ulnar/radial deviation. A wooden insert was added to the brace to ensure that the hand is unable to flex/extend. To restrict pronation/supination, the brace was affixed to a padded elbow brace with an articulated joint (Orthomen ROM Elbow Brace) using a bolt and Velcro. Although the elbow brace is commonly used to restrict elbow movement to a certain range, the brace was left in its full range of motion configuration. This composition of braces achieves the additional constraining of the wrist along the pronation/supination axis. The majority of prior work in this area that have used a wrist brace do not limit pronation/supination (e.g. [2], [8], [17]).

Figure 6: Motion capture marker configuration on an amputee participant, using a combination of marker clusters (attached to flexible sheet plastic) and individual markers.

B. Study Procedure

Reaching tasks required the participants to begin with their torsos laterally aligned with the central pole of the grid, standing at a distance of 0.6m away. Marks were placed on the floor to help keep participants aligned throughout the experiment. Participants were instructed to begin and end each reaching motion with their arms relaxed by their sides. They were requested to reach to each target one at a time and squeeze the target with a power grasp. Reaching motions were to start at the top right location working their way across the entire row before moving down to the next row starting with the rightmost target once again. If using the left arm, reaching motions were to progress left to right instead. Participants were instructed to avoid stepping unless it was necessary and ensure that their feet returned to the starting position after each grasp. Failure to return the arm or feet to the starting position prompted a repeat of the reaching movement; this was to ensure that each reach began from the same pose.

Able-bodied participants reached towards the 49 targets on the grid a total of six times: in both vertical and horizontal orientations of the grid with three wrist mobility conditions, i.e. unrestrained, while wearing a 2DOF wrist brace (limits flexion/extension and ulnar/radial deviation), and while wearing the 3DOF wrist brace (additionally limits pronation/supination). Prosthesis users reached towards the targets only four times; in both grid orientation participants used their dominant hand and their transradial device. Both prosthesis users had the ability to pronate/supinate their wrist, however, only one had a powered wrist device. The amputee participant with the powered wrist (P8) was instructed to begin their motions with their wrist in a neutral position, while the other amputee participant (P9) was allowed to manually rotate their wrist prior to starting the reaching.

It took approximately 30 minutes to outfit each participant with ~~the~~ motion capture markers and allow them time to get used to the task; this was particularly important for the participants that donned the wrist braces. The grid reaching

procedure took an additional 20-30 minutes (in total, for all conditions).

In summary, the study involved the following variation in conditions:

- Target orientation:
  - Horizontal / Vertical
- Wrist brace condition (intact participants)
  - Unimpaired / 2DOF / 3DOF
- Limb used (amputee participants)
  - Intact / Affected

C. Participants

A total of 9 (5 male, 4 female) subjects were enrolled in this study, 2 (1 male, 1 female) of which were transradial prosthesis users both with one fully intact limb (see Table 1). Participants spanned the ages of 23-56. An initial screening was made to ensure that participants had no other motion or vision impairments that would interfere with the data collection.

Table 1. Attributes of the nine participants. Weight is in lbs. 'Dom. Hand' is an abbreviation of dominant hand. Arm length is measured from the shoulder to the tip of the middle finger. P8 and P9 were prosthesis users, and the lengths of both arms are therefore reported.

Participant	Sex	Age	Weight (kg)	Height (ft/m)	Dom. Hand	Dom. Arm Length (m)	Pros. Arm Length (m)
P1	F	24	125	5'6.5"/1.68	R	28"0.71	
P2	M	29	185	6'2"/1.88	R	27"0.66	
P3	M	24	160	5'8"/1.73	R	24"0.61	
P4	M	56	175	5'10"/1.78	R	27.5"0.70	
P5	F	55	134	5'6"/1.68	R	27.5"0.70	
P6	F	38	156	5'6"/1.68	R	29.2"0.74	
P7	M	46	165	5'8"/1.73	R	29"0.74	
P8	M	53	210	6'1"/1.85	R	30.4"0.77	28"0.71
P9	F	23	135	5'9"/1.75	L	26.5"0.67	22.2"0.56

IV. Data Processing

A. Data structure

Motion capture data was processed in Vicon Bodybuilder and MATLAB 2021a and converted to establish co-ordinate frames at the center of the wrist, elbow, and shoulder. From this, joint angles were obtained according to ISB (International Society on Biomechanics) standards [22]. Joint angles of the left arm were calculated such that joint angle trajectories were analogous to the right arm.

Co-ordinate frames were additionally created for the head, thorax, and pelvis to enable the extraction of Cartesian position data C and joint angles θ, as listed in Table 2.

Table 2. Joint angle and body segment nomenclature. Shaded wrist angles have their motion restricted in the impaired test conditions.

Trunk		Shoulder		Body Segments	
θ_{TX}	Flexion	θ_{SX}	Plane of Elevation	C_{Th}	Thorax Center
θ_{TY}	Rotation	θ_{SY}	Elevation	C_{Sh}	Shoulder Center
θ_{TZ}	Lateral Flexion	θ_{SZ}	Internal Rotation	C_{el}	Elbow Center
Elbow		**Wrist**		C_{Wr}	Wrist Center
θ_{EL}	Elbow Flexion	θ_{WX}	Pronation/Suppination		
		θ_{WY}	Flexion / Extension		
		θ_{WZ}	Radial/Ulnar Deviation		

Each set of 49 reaching motions (to all points on the grid) were captured in a single recording. Due to the high volume of trials, automatic segmentation of reaching motions was performed in MATLAB by the method described in Fig. 7. First the Y-velocity of the wrist segment was analysed for peaks and points of threshold crossing (the threshold was set at 0.2 mm/sample). Trajectories could only be identified between a positive and negative velocity threshold crossing (Fig. 8). By factoring velocity and not just position, we ensure that later

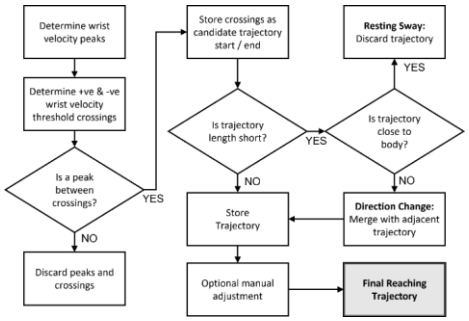

Figure 7: Reaching motion interval determination process.

mean angle calculations do not incorporate periods before or after reaching motions, when the participant dwells in a given pose. Candidate trajectories identified by this measure were then tested for trajectory length and proximity to the body, to automatically reject arm swaying motions while the participant was stationary. As some sub-motions confounded our automatic algorithm, all automatically determined trajectories were visually inspected and manually corrected if necessary. Fig. 9 shows the resulting set of 49 wrist-center reaching trajectories for participant P1 with brace 1 for horizontal grasps. A complete set of 6 trajectory illustrations captured by P1 for all brace and orientation conditions is provided in the appendix (Fig. 13), while all trajectories for all participants are available in the accompanying dataset.

B. Metrics

The chosen metrics (mean angle, range of motion and trajectory length) were intended to capture relevant variations in reaching patterns and so were applied to each reaching motion. Mean angle and range of motion (ROM) are typical metrics used in evaluating reaching (e.g. in [8] and [15] respectively), where larger values are often associated with compensatory motion. However, neither metric directly captures the length of the path that a joint center takes, which may differ substantially between reaching conditions. Following this consideration, we additionally evaluate the length of the Cartesian path that the wrist joint centers traverses.

1) Mean Angle

Mean angle M was calculated for each of the 7 joint angles θ_n (n=1 to 7), corresponding to the torso, shoulder and elbow (Table 2). An unweighted average is obtained using the angle values achieved during a reaching motion:

Formatted: List Paragraph, Bulleted + Level: 2 + Aligned at: 0.89" + Indent at: 1.14"

$$M_n = \frac{\sum_{i=1}^{m} \theta_{ni}}{m}$$

where i is the sample, and m is the number of samples in the trajectory.

2) Difference in Range of Motion (dROM)

We track and measure the ROM of the 7 joint angles corresponding to the torso, shoulder, elbow, and wrist (Table 2). ROM is calculated as:

$$R_\theta = \max(\theta_n) - \min(\theta_n)$$

3) Trajectory Length

The trajectory lengths L of each joint center (thorax, shoulder, elbow, and wrist) is computed as the sum of Euclidean distances traversed by the joint center:

$$L = \sum_{i=1}^{m} \sqrt{|X_i - X_{i+1}|^2 + |Y_{ci} - Y_{i+1}|^2 + |Z_i - Z_{i+1}|^2}$$

where (X_i, Y_i, Z_i) is the Cartesian coordinate of a joint center, i is the sample, and m is the number of samples in the reaching motion. This metric is calculated for the wrist joint center.

V. Results

A total of 2450 individual reaching motions were recorded (2058 able-bodied and 392 amputee). The metrics discussed in Section IV were applied to each reaching motion. The motions were then averaged between participants to get an overall reaching motion pattern for each condition. Those averaged results have been visualized via spatially relevant heat maps, using the MATLAB command *imagesc*. In these plots, each grid square represents motion associated with reaching to the corresponding grid target, as 'viewed' from the perspective of the participant (Fig. 3). In the case of left arm reaching, which involved the participants progressing from the top left target instead of top right (Section III.B), the columns of the data were flipped left to right, giving consistency in the generated heat maps. The~~se~~ heat-maps have been illustrated in Fig. 10-12 and Fig. 14 in the appendix.

As it is challenging to integrate the various differences of the numerous metrics and conditions presented in these heat-maps, we also applied principal component analysis (PCA) to each metric, plotting the result of the component with greatest variance in Fig. 12.

The ~~numeric~~ scalar values ~~outputs of the~~ that make up the heat-maps were subjected to statistical testing across different conditions via a paired t-test (so that each position on the grid was associated with its spatial counterparts) using the ~~Matlab~~MATLAB command *ttest2*. ~~with~~ Bonferroni correction was applied. This allowed a definitive cross-condition comparison, as illustrated in Table 3.

VI. Discussion

A. Heat Map Representation

To pursue generalizable results, this work recorded and processed a large number (2,450) of reaching motions over several conditions (as described in Section III.B). Given the many trajectories and variables, conventional methods of illustrating motion differences (e.g. XY plots of joint angle vs time as in [2], [8]) were deemed as infeasible for this dataset. We instead pursued heat maps, which represent the spatial relationship of a scalar variable (such as trunk flexion range of

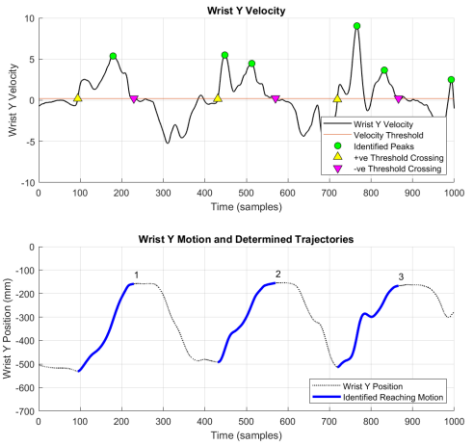

Figure 8: Automatic reaching trajectory determination using velocity based peaks and threshold crossings.

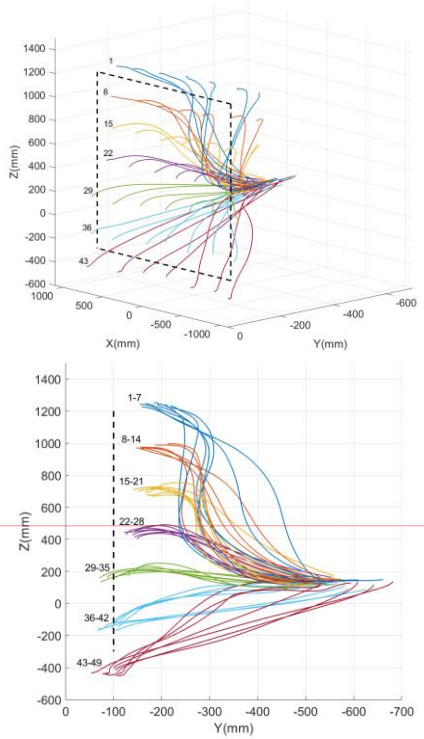

Figure 9: Wrist position for all 49 reaching trajectories for participant P1 performing horizontal grasps with brace 1, in isometric and side views. The Y axes are at different scales to highlight trajectory variation. The colours specify the row of the target grid.

Formatted: Font: Italic

Formatted: Normal, Justified, No bullets or numbering

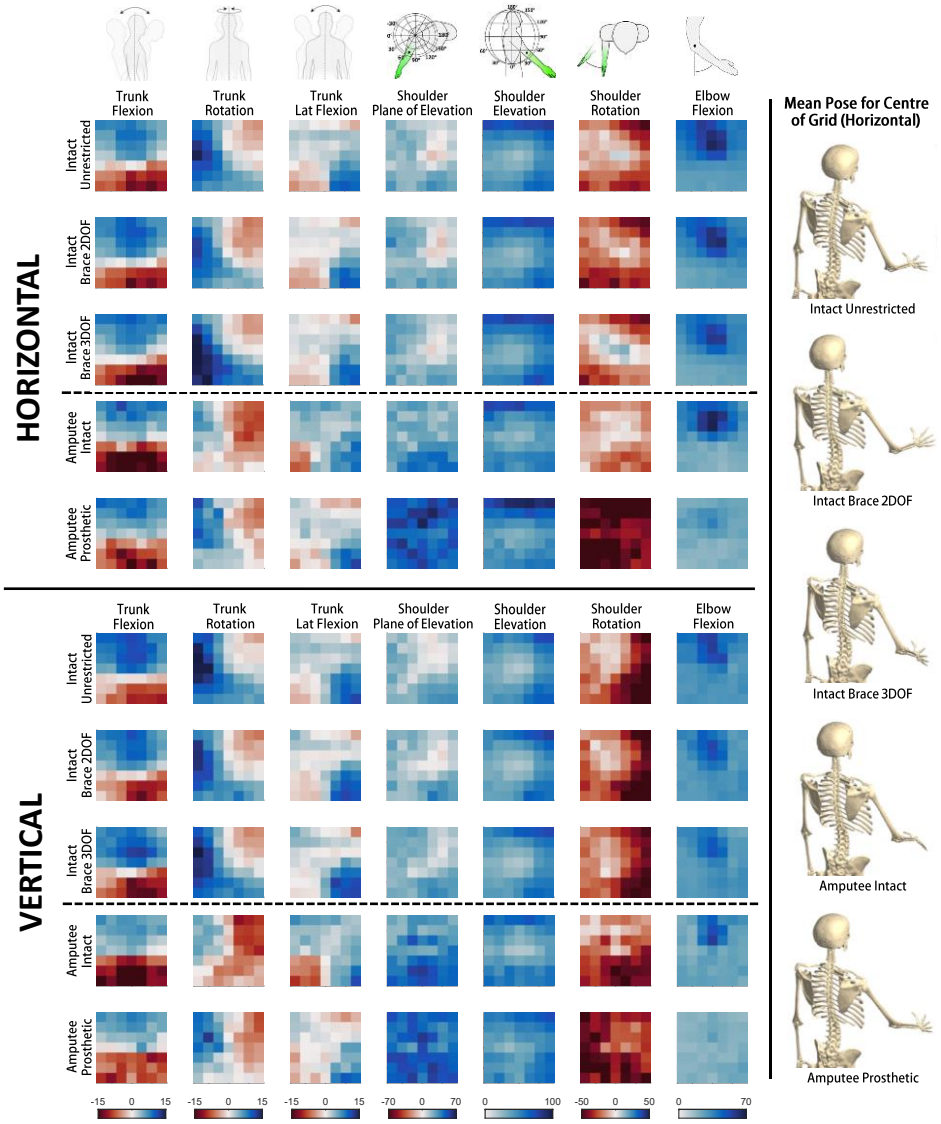

Figure 10: Mean joint angles for horizonal and vertical reaching tasks. Units are in degrees. Skeleton images illustrate changes in average pose for reaching to the center target of the grid for the horizontal condition. The spatial layout of the reaching grid can be observed in Fig. 3

motion) over the 2D workspace (Fig. 3). To interpret the heatmaps, one may look at patterns of how a variable increases or decreases as participants reached to the different target locations. For example, in Fig. 10 it may be observed that the mean joint angle of trunk flexion observes a linearly separable trend (as users bend backwards or forwards to reach different height targets. For comparison, trunk rotation observes a more radial pattern, with the greatest negative values in the top right corner. Within each figure, the separate heat maps represent different variables (e.g. joints, body segments) and study conditions.

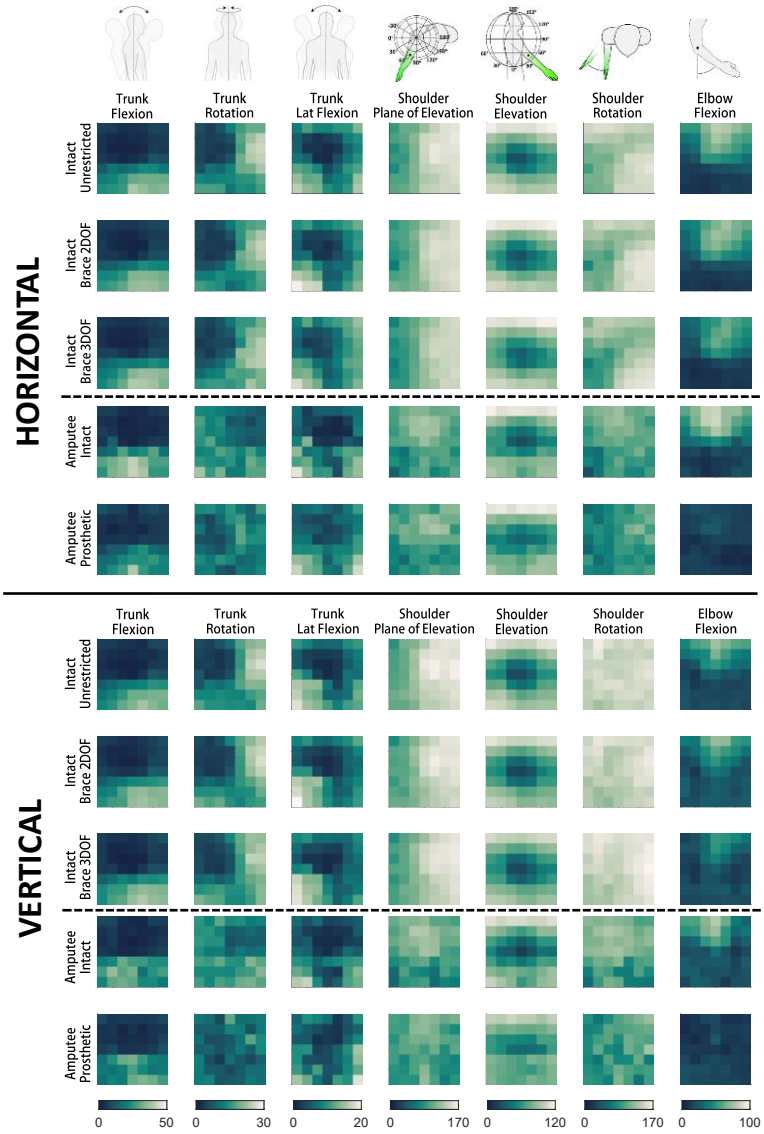

Figure 11: Range of Motion for horizonal and vertical reaching tasks. Units are in degrees.

~~A.~~B. *Mean Angle*

Reaching is a movement that couples arm and body joints~~,~~ and analyzing them independently has revealed unexpected patterns. Referencing the first two columns of Fig. 10, ~~T~~trunk flexion and rotation appear to be the dominant factor when reaching across the grid, more so than the shoulder, something that was also observed in ADL tasks [23]. Trunk flexion and rotation are positively correlated to marker height and contralateral location, respectively, and the trend is consistent across all participants. Trunk flexion pattern across the grid is similar for all conditions as well (Table 3). However, shoulder

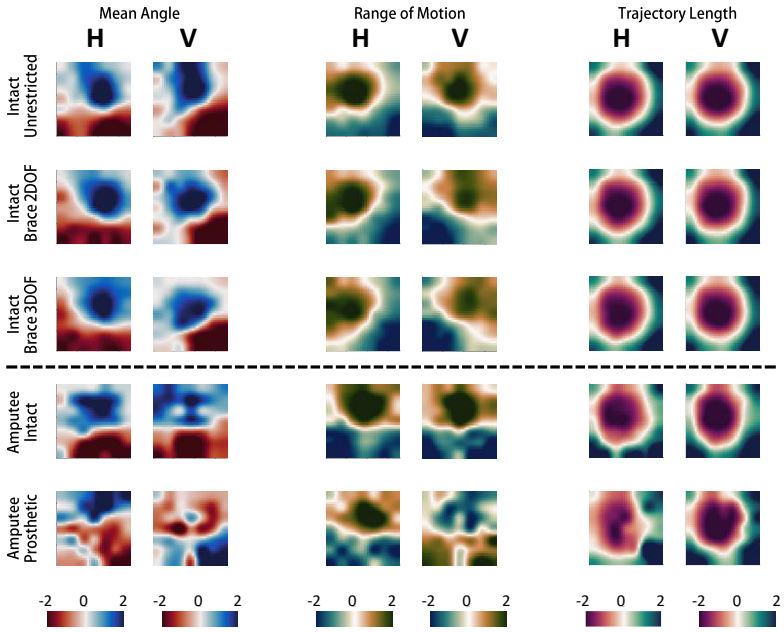

Figure 12: Principal Component Analysis of the three metrics. To highlight spatial trends, bicubic interpolation was implemented (n=5).

plane of elevation (fourth column) remains largely the same across the grid (for all conditions), and is particularly evident in the amputee participants (both arms). Likewise, shoulder elevation (fifth column) appears to be highest towards the middle of the grid, suggesting that other joints begin to overcompensate when reaching for higher locations on the grid, such as trunk lateral flexion.

Several expectations are also confirmed. Joint patterns appear to only gradually change when going from the unrestricted to the brace 2DOF to the brace 3DOF conditions; observed by the lack of significant difference in the first three rows of the mean angle results in Table 3 for both horizontal and vertical conditions. Reaching to the grid in its horizontal orientation has exaggerated the mean angle patterns in the trunk and shoulder when compared to the vertical orientation; joints had a greater range of mean values (Fig. 10). We also see that the joint angle patterns of the unrestricted case of the normative population is more akin to the intact limb of the amputee population than the prosthesis case. For example, shoulder elevation is needed to orient the end effector horizontally when the wrist is unable to supinate~~restricted~~, and ~~thus~~ we would ~~explain why~~ expect the prosthesis and 3DOF braced conditions ~~to appear to~~ have larger mean shoulder elevation and ~~smaller mean forearm pronation~~rotation; while visually this appears to be the case (Fig. 10), only shoulder rotation was significantly different (Table 3). This coupling also validates a previous prosthesis control development [24].

Both the intact limb and prosthesis of the amputee participants appear to have an unusual, yet similar, trunk rotation pattern, reinforcing the idea that living with limb difference has an impact on the intact limb as well [25]. Another notable observation is that the prosthetic limb did not consistently match the patterns observed in the 3DOF brace case. For example, it appears that the elbow hardly flexes when reaching with the prosthetic limb (Fig. 10, seventh column). Since the same number of wrist-DOF were restricted, a likely explanation for the observed difference is that finger dexterity enabled the normative participants to grasp the markers even if the hand was not perfectly aligned with the target. Another explanation is the lack of prosthesis embodiment when compared to the intact limb, even if restricted with a brace.

~~B.~~C. *Range of Motion*

Because the observed joint ROM is correlated with mean joint angle, several takeaways overlap with the prior section, as is seen in Table 3. As the bracing conditions become more restrictive (going from 2DOF to 3DOF), we ~~expected to see~~observed more body compensation (i.e. increased shoulder rotation ROM), though the differences were not statistically significant ~~and yet, very little difference was observed~~(first three rows of ROM results in Table 3). However, statistically, the lack of supination did significantly affect shoulder rotation of amputees when reaching horizontally (Table 3, last row). The shoulder ROM did not compensate for reaching of the amputee participants for either of their limbs as it did for all the conditions of the normative participants; visually observed as a difference in ROM values across the grid between the populations (Fig. 11, fourth-sixth columns). This, again,

reinforcesing the idea that limb difference affects even the intact limb. Here, lack of elbow flexion in the prosthesis use case is even more apparent (Fig. 11, last row seventh column).

C.D. *Trajectory Length*

Unsurprisingly, the trajectory path length was generally lowest when reaching towards the center of the grid for all joints (Fig. 14). The region of the grid that resulted in the least amount of travel for the thorax and the shoulder was slightly higher than for the elbow and wrist. However, the precise pattern across the grid is likely affected by arm length and standing distance from the grid, and thus only represents our participant pool. The added supination restriction in the 3DOF brace did not appear to significantly impact trajectory length of any of the body segments over the 2DOF case as we initially expected.

Differences between prosthesis use and the normative population were further exaggerated in the horizontal case (Fig. 14). For the horizontal condition, thorax travel distance was significant between prosthesis use and the intact limb and the braced 2DOF case, while it was not significantly different than the 3DOF case (Table 3). This suggests that the 3DOF brace achieves some amount of emulation of a prosthesis that lacks wrist controllability.

Table 3: T-Tests with Bonferroni correction, p = 0.05/8 = 0.00625. All significant differences have been highlighted in blue.

Mean Angle Horizontal

	Trunk X	Trunk Y	Trunk Z	Shoulder X	Shoulder Y	Shoulder Z	Elbow
Intact / Brace 1	0.418	0.150	0.287	0.564	0.884	0.049	0.538
Intact / Brace 2	0.943	0.223	0.707	0.275	0.197	0.079	0.043
Brace 1 / Brace 2	0.412	0.014	0.477	0.655	0.238	4.29E-04	0.147
Intact / Amputee (Un)	0.158	5.11E-09	0.111	4.96E-09	0.855	2.63E-03	6.86E-02
Intact / Amputee (Pros)	0.778	0.015	0.635	3.71E-36	0.146	1.12E-22	1.02E-13
Brace1 / Amputee (Pros)	0.289	0.351	0.534	1.16E-32	0.176	4.60E-19	4.61E-13
Brace 2 / Amputee (Pros)	0.848	8.15E-04	0.922	8.52E-35	0.787	3.39E-24	4.20E-10
Amputee (Un) / Amputee (Pros)	0.249	1.46E-04	0.038	8.03E-23	0.092	7.43E-35	1.75E-06

Mean Angle Vertical

	Trunk X	Trunk Y	Trunk Z	Shoulder X	Shoulder Y	Shoulder Z	Elbow
Intact / Brace 1	0.387	0.104	0.398	0.700	0.943	0.413	0.144
Intact / Brace 2	0.365	0.469	0.951	0.020	0.862	0.698	0.012
Brace 1 / Brace 2	0.912	0.405	0.460	0.048	0.923	0.614	0.273
Intact / Amputee (Un)	1.53E-03	4.47E-13	0.231	1.29E-15	0.407	0.942	2.60E-05
Intact / Amputee (Pros)	0.010	2.18E-05	0.008	2.50E-31	0.044	1.60E-04	1.90E-22
Brace1 / Amputee (Pros)	0.082	6.64E-03	0.102	2.80E-31	0.065	2.95E-03	1.89E-22
Brace 2 / Amputee (Pros)	0.139	6.96E-04	0.016	3.56E-30	0.071	1.14E-04	6.19E-23
Amputee (Un) / Amputee (Pros)	0.265	2.79E-04	0.286	5.56E-07	0.252	2.06E-05	6.97E-09

ROM Horizontal

	Trunk X	Trunk Y	Trunk Z	Shoulder X	Shoulder Y	Shoulder Z	Elbow
Intact / Brace 1	0.787	0.581	0.744	0.624	0.958	0.441	0.900
Intact / Brace 2	0.728	0.790	0.235	0.068	0.806	0.002	0.093
Brace 1 / Brace 2	0.933	0.406	0.413	0.172	0.766	0.024	0.108
Intact / Amputee (Un)	0.689	0.694	0.226	5.01E-09	0.403	9.85E-18	0.527
Intact / Amputee (Pros)	0.421	0.073	0.969	4.73E-11	0.499	4.80E-28	3.11E-09
Brace1 / Amputee (Pros)	0.275	0.245	0.698	4.50E-10	0.538	1.01E-22	1.02E-09
Brace 2 / Amputee (Pros)	0.249	0.030	0.183	1.36E-06	0.342	1.47E-15	5.56E-07
Amputee (Un) / Amputee (Pros)	0.245	0.038	0.210	0.264	0.852	3.26E-04	6.38E-10

ROM Vertical

	Trunk X	Trunk Y	Trunk Z	Shoulder X	Shoulder Y	Shoulder Z	Elbow
Intact / Brace 1	0.613	0.927	0.925	0.383	0.473	0.090	0.679
Intact / Brace 2	0.709	0.699	0.766	0.309	0.309	0.266	0.018
Brace 1 / Brace 2	0.902	0.771	0.696	0.873	0.773	0.021	0.002
Intact / Amputee (Un)	0.932	0.569	0.038	1.01E-11	0.301	2.64E-24	0.509
Intact / Amputee (Pros)	0.812	0.001	0.390	1.91E-15	0.509	1.10E-39	5.40E-10
Brace1 / Amputee (Pros)	0.436	0.001	0.340	5.67E-13	0.852	9.66E-35	5.66E-14
Brace 2 / Amputee (Pros)	0.529	1.65E-04	0.584	4.23E-12	0.594	4.73E-37	5.02E-09
Amputee (Un) / Amputee (Pros)	0.882	9.82E-09	0.180	0.471	0.572	3.62E-04	1.48E-11

Distance Horizontal

	Trunk	Shoulder	Elbow	Wrist
Intact / Brace 1	0.907	0.911	1.000	0.534
Intact / Brace 2	0.727	0.764	0.902	0.591
Brace 1 / Brace 2	0.817	0.854	0.903	0.939
Intact / Amputee (Un)	0.715	0.219	1.47E-07	2.81E-11
Intact / Amputee (Pros)	0.003	0.302	0.002	1.39E-05
Brace1 / Amputee (Pros)	0.005	0.364	0.002	8.95E-07
Brace 2 / Amputee (Pros)	0.008	0.456	0.001	1.79E-06
Amputee (Un) / Amputee (Pros)	0.013	0.015	0.016	0.003

Distance Vertical

	Trunk	Shoulder	Elbow	Wrist
Intact / Brace 1	0.903	0.964	0.863	0.840
Intact / Brace 2	0.853	0.877	0.635	0.992
Brace 1 / Brace 2	0.950	0.840	0.761	0.852
Intact / Amputee (Un)	0.687	0.451	1.06E-06	1.41E-10
Intact / Amputee (Pros)	0.056	0.829	2.90E-04	3.13E-08
Brace1 / Amputee (Pros)	0.071	0.865	0.001	3.96E-08
Brace 2 / Amputee (Pros)	0.078	0.702	0.002	8.75E-08
Amputee (Un) / Amputee (Pros)	0.140	0.311	0.185	0.224

D.E. *PCA*

PCA revealed and summarized the primary patterns of motion, accounting for all joints simultaneously, making comparison across the different conditions more generalizable (Fig. 12). For example, it is apparent that the prothesis reaching mean angle and ROM is less regular across the different grid locations, suggesting that it may be less predictable (last row). It can also be seen that it is less like the normative population, including the brace conditions, than even when comparing reaching with the intact limb. Trajectory path length did not significantly vary between the conditions (Fig. 12, last two columns), meaning that body compensation predominantly occurs in the posture, though it does reveal which regions of the grid result in greater exertion (outer edge).

VII. Conclusion

In this work we investigated the impact of wrist mobility on body compensation when reaching towards a grid of discretized horizontal and vertical target locations. We emulated a lack of wrist mobility in prosthesis users using two braces, one that limits wrist pronation and flexion, and one that additionally limits supination. Observations were then compared to two prosthesis users with several notable findings. Since the amputee participants had wrist rotators, their performance was expected to match that of the 2DOF wrist brace, and while imperfect, the braces emulated some aspects of prosthesis users. Discrepancies could be attributed to several factors, such as differences in limb lengths between the intact limb and the prosthesis, as well as a lack of grasping adaptability, i.e. compliant fingers in healthy people could have compensated for the absence of wrist deviation while the prosthetic hands could not. By studying reaching with the intact limb of the amputees, it was also evident that the effects of the amputation were not limited to the affected arm alone.

Studying reaching across a discretized space revealed patterns of movement and compensation that statistics could not do alone. For example, reaching contralaterally was largely driven by torso movement rather than shoulder while PCA revealed regions of greater exertion. The results presented here should be used to guide therapists in understanding which areas of the workspace have higher motion demands on different aspects of the body.

References

[1] N. M. Bajaj, A. J. Spiers, and A. M. Dollar, “State of the art in prosthetic wrists: Commercial and research devices,” in *IEEE International Conference on Rehabilitation Robotics*, 2015, vol. 2015-Septe, pp. 331–338, doi: 10.1109/ICORR.2015.7281221.

[2] F. Montagnani, M. Controzzi, and C. Cipriani, “Is it Finger or Wrist Dexterity That is Missing in Current Hand Prostheses?,” *IEEE Trans. Neural Syst. Rehabil. Eng.*, vol. 21, no. c, pp. 1–1, 2015, doi: 10.1109/TNSRE.2015.2398112.

[3] A. Hussaini, A. Zinck, and P. Kyberd, “Categorization of compensatory motions in transradial myoelectric prosthesis users,”

Prosthet. Orthot. Int., 2016, doi: 10.1177/0309364616660248.

[4] A. Kato, H. Nagumo, M. Tamon, M. G. Fujie, and S. Sugano, "Evaluation of Compensatory Movement by Shoulder Joint Torque during Gain Adjustment of a Powered Prosthetic Wrist Joint," *Proc. Annu. Int. Conf. IEEE Eng. Med. Biol. Soc. EMBS*, vol. 2018-July, pp. 1891–1894, 2018, doi: 10.1109/EMBC.2018.8512594.

[5] M. D. Paskett *et al.*, "A Modular Transradial Bypass Socket for Surface Myoelectric Prosthetic Control in Non-Amputees," *IEEE Trans. Neural Syst. Rehabil. Eng.*, vol. 27, no. 10, pp. 2070–2076, 2019, doi: 10.1109/TNSRE.2019.2941109.

[6] N. R. Olsen *et al.*, "An Adaptable Prosthetic Wrist Reduces Subjective Workload," *bioRxiv*, 2019, doi: 10.1101/808634.

[7] A. Matias, C. Bennett, S. Estelle, J. L. Roper, and B. W. Smith, "Biomechanical Comparison of the Validity of Two Configurations of Simulators for Body-Powered Hand Prostheses," *Proc. IEEE RAS EMBS Int. Conf. Biomed. Robot. Biomechatronics*, vol. 2020-Novem, pp. 422–427, 2020, doi: 10.1109/BioRob49111.2020.9224379.

[8] A. G. Mell, B. L. Childress, and R. E. Hughes, "The effect of wearing a wrist splint on shoulder kinematics during object manipulation.," *Arch. Phys. Med. Rehabil.*, vol. 86, no. 8, pp. 1661–4, Aug. 2005, doi: 10.1016/j.apmr.2005.02.008.

[9] M. Deijs, R. M. Bongers, N. D. M. Ringeling-Van Leusen, and C. K. Van Der Sluis, "Flexible and static wrist units in upper limb prosthesis users: Functionality scores, user satisfaction and compensatory movements," *J. Neuroeng. Rehabil.*, vol. 13, no. 1, 2016, doi: 10.1186/s12984-016-0130-0.

[10] Q. Wan, R. P. Adams, and R. D. Howe, "Variability and predictability in tactile sensing during grasping," *Proc. - IEEE Int. Conf. Robot. Autom.*, vol. 2016-June, pp. 158–164, 2016, doi: 10.1109/ICRA.2016.7487129.

[11] A. J. Spiers, Y. Gloumakox, and A. M. Dollar, "Examining the Impact of Wrist Mobility on Reaching Motion Compensation Across a Discretely Sampled Workspace," *Proc. IEEE RAS EMBS Int. Conf. Biomed. Robot. Biomechatronics*, vol. 2018-Augus, pp. 819–826, 2018, doi: 10.1109/BIOROB.2018.8487871.

[12] T. Kang, J. He, and S. I. H. Tillery, "Determining natural arm configuration along a reaching trajectory," *Exp. Brain Res.*, vol. 167, no. 3, pp. 352–361, 2005, doi: 10.1007/s00221-005-0039-5.

[13] A. Spiers, S. G. Khan, and G. Herrmann, *Biologically inspired control of humanoid robot arms: Robust and adaptive approaches*. 2016.

[14] A. Murgia, P. Kyberd, and T. Barnhill, "The use of kinematic and parametric information to highlight lack of movement and compensation in the upper extremities during activities of daily living," *Gait Posture*, vol. 31, no. 3, pp. 300–306, 2010, doi: 10.1016/j.gaitpost.2009.11.007.

[15] M. J. Major, R. L. Stine, C. W. Heckathorne, S. Fatone, and S. a Gard, "Comparison of range-of-motion and variability in upper body movements between transradial prosthesis users and able-bodied controls when executing goal-oriented tasks.," *J. Neuroeng. Rehabil.*, vol. 11, no. 1, 2014, doi: 10.1186/1743-0003-11-132.

[16] S. L. Carey, M. Jason Highsmith, M. E. Maitland, and R. V Dubey, "Compensatory movements of transradial prosthesis users during common tasks.," *Clin. Biomech. (Bristol, Avon)*, vol. 23, no. 9, pp. 1128–35, Nov. 2008, doi: 10.1016/j.clinbiomech.2008.05.008.

[17] B. D. Adams, N. M. Grosland, D. M. Murphy, and M. McCullough, "Impact of impaired wrist motion on hand and upper-extremity performance," *J. Hand Surg. Am.*, vol. 28, no. 6, pp. 898–903, 2003, doi: 10.1016/S0363-5023(03)00424-6.

[18] C. M. Light, P. H. Chappell, and P. J. Kyberd, "Establishing a standardized clinical assessment tool of pathologic and prosthetic hand function: Normative data, reliability, and validity," *Arch. Phys. Med. Rehabil.*, vol. 83, no. 6, pp. 776–783, 2002, doi: 10.1053/apmr.2002.32737.

[19] N. M. Bajaj and A. M. Dollar, "Design and Preliminary Evaluation of a 3-DOF Powered Prosthetic Wrist Device," *Proc. IEEE RAS EMBS Int. Conf. Biomed. Robot. Biomechatronics*, vol. 2018-Augus, pp. 119–125, 2018, doi: 10.1109/BIOROB.2018.8487192.

[20] P. J. Kyberd *et al.*, "Two-degree-of-freedom powered prosthetic wrist," *J. Rehabil. Res. Dev.*, vol. 48, no. 6, p. 609, 2011, doi: 10.1682/JRRD.2010.07.0137.

[21] Y. Gloumakov, J. Bimbo, and A. M. Dollar, "Trajectory Control-An Effective Strategy for Controlling Multi-DOF Upper Limb Prosthetic Devices," *IEEE Trans. Neural Syst. Rehabil. Eng.*, vol. 30, pp. 420–430, 2022, doi: 10.1109/TNSRE.2022.3151055.

[22] G. Wu *et al.*, "ISB recommendation on definitions of joint coordinate systems of various joints for the reporting of human joint motion - Part II: Shoulder, elbow, wrist and hand," *J. Biomech.*, vol. 38, no. 5, pp. 981–992, 2005, doi: 10.1016/j.jbiomech.2004.05.042.

[23] Y. Gloumakov, A. J. Spiers, and A. M. Dollar, "Dimensionality Reduction and Motion Clustering during Activities of Daily Living: Decoupling Hand Location and Orientation," *IEEE Trans. Neural Syst. Rehabil. Eng.*, vol. 28, no. 12, pp. 2955–2965, 2020, doi: 10.1109/TNSRE.2020.3040716.

[24] D. A. Bennett and M. Goldfarb, "IMU-Based Wrist Rotation Control of a Transradial Myoelectric Prosthesis," *Trans. Neural Syst. Rehabil. Eng.*, no. 99, 2016, doi: 10.1109/TNSRE.2017.2682642.

[25] S. G. Postema *et al.*, "Musculoskeletal Complaints in Transverse Upper Limb Reduction Deficiency and Amputation in the Netherlands: Prevalence, Predictors, and Effect on Health," *Arch. Phys. Med. Rehabil.*, vol. 97, no. 7, pp. 1137–1145, 2016, doi: 10.1016/j.apmr.2016.01.031.

VIII. APPENDIX

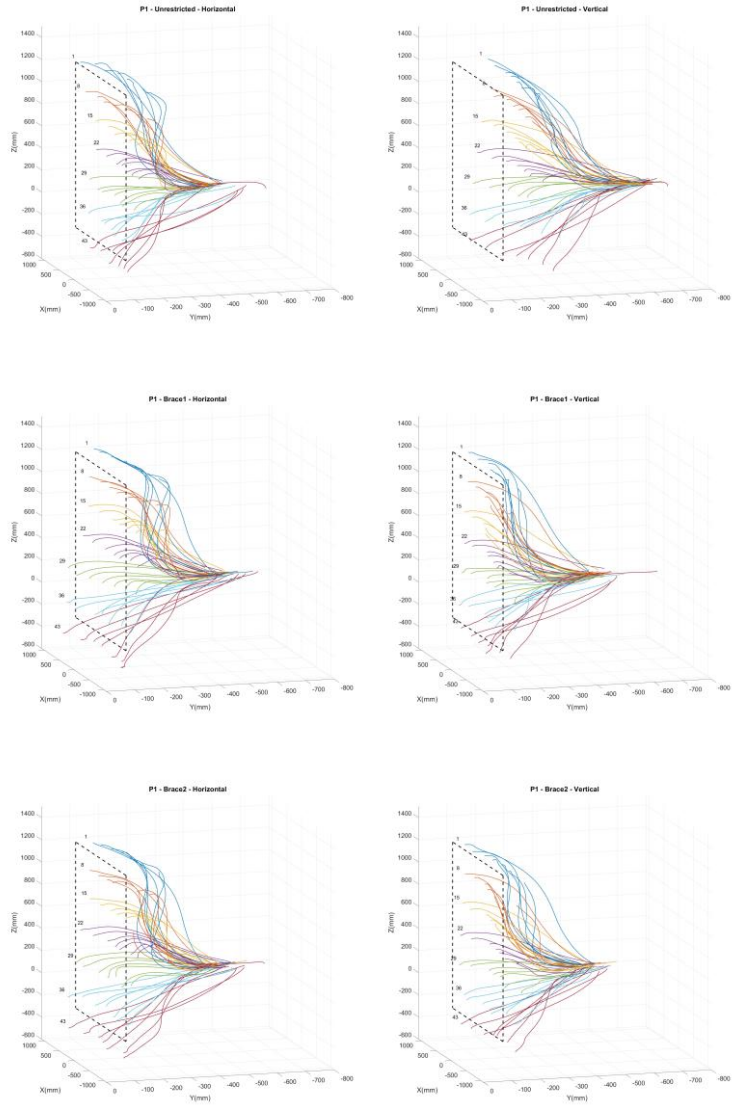

Figure 13: All recorded reaching trajectories for participant P1

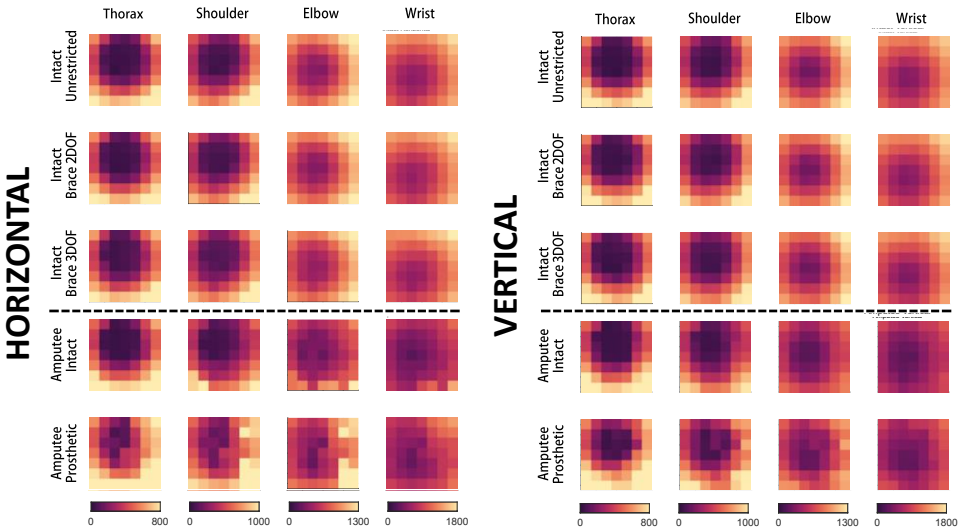

Figure 14: Trajectory length reaching result. The units are mm.